Computational Materials Science 112 (2016) 448–458

Contents lists available at ScienceDirect

Computational Materials Science

journal homepage: www.elsevier.com/locate/commatsci

Microscopic mechanism of spin-order induced improper ferroelectric polarization

P.S. Wang [a], X.Z. Lu [b], X.G. Gong [a], H.J. Xiang [a,*]

[a] Key Laboratory of Computational Physical Sciences (Ministry of Education), State Key Laboratory of Surface Physics, Collaborative Innovation Center of Advanced Microstructures, and Department of Physics, Fudan University, Shanghai 200433, PR China
[b] Department of Materials Science and Engineering, Northwestern University, Evanston, IL 60208, USA

ARTICLE INFO

Article history:
Received 8 June 2015
Received in revised form 14 August 2015
Accepted 19 August 2015
Available online 29 October 2015

Keywords:
Multiferroics
Density functional theory

ABSTRACT

Type-II multiferroic is an important area in the big family of multiferroics, in which its polarization originates from the spin order, resulting in a strong magnetoelectric coupling. Here we briefly review the previous mechanisms of the spin-order induced polarization, including the Katsura–Nagaosa–Balatsky (KNB) model, inverse Dzyaloshinskii-Moria (DM) interaction model, exchange striction model, and the bond polarization model. Then our unified polarization model is discussed in detail, which contains pure electronic, ion displacement and lattice deformation contributions. And a feasible approach for constructing the unified model based on the first-principles calculations is presented. With this model, we unravel the microscopic mechanisms of the ferroelectricity in several typical multiferroics. New type-II multiferroics with strong magnetoelectric coupling and giant polarization are expected to be discovered and/or designed through the use of this model.

1. Introduction

Multiferroics [1–7], in which magnetism, ferroelectricity and ferroelasticity can coexist, have attracted great interest in the last decades, not only for their fascinating physics but also for their potential applications in memory devices, spintronics and magnetoelectric sensors, etc. Multiferroicity occurs in both single phase and composite materials. In composite multiferroics [8–12], the magnetoelectric effect is usually generated as a product property of a magnetostrictive and a piezoelectric substance. Hereafter we only discuss the single phase multiferroics. Multiferroics are found from 3d to 4f transition metal compounds and have perovskite structures, spinel structures or pyrochlore structures, etc. The magnetism in multiferroics almost has the same origin: The partially filled d or f shells of transition metal or rare earth ions. The mechanism of the origin of the ferroelectric polarization is more complicated. Khomskii [13] defines two types of multiferroics. Type-I multiferroics are the materials in which ferroelectricity and magnetism have different sources and appear largely independent of one another. The coupling between the magnetism and ferroelectricity in type-I multiferroics is usually weak. The representative type-I multiferroics are Zn_2FeTaO_6 and Zn_2FeOsO_6 [14], $PbVO_3$ [15], $BiFeO_3$ [16], $BiMnO_3$ [17], and $YMnO_3$ [18], etc. While in type-II multiferroics, the ferroelectricity originates from special spin orders: cycloid, proper screw, etc. The magnetic order breaks the inversion symmetry in type-II multiferroics. Thus one would expect strong magnetoelectric coupling in type-II multiferroics, which provides a promising route for electrical writing and nondestructive magnetic readout memory devices. This new type of memory devices has the advantages of high storage density, high read-write speed and low energy consumption. The representative type-II multiferroics are $TbMnO_3$ [19], $DyMnO_3$ [20], $TbMn_2O_5$ [21] and $CaMn_7O_{12}$ [22,23], etc.

The magnetoelectric coupling in type-II multiferroics is much stronger than that in type-I multiferroics. However, the polarization in most known type-II multiferroics is much smaller than the traditional type-I multiferroics. This limits the realistic applications of type-II multiferroics. Therefore, discovering and/or designing new type-II multiferroics with large polarization is an active and important research area. To gain insight into the mechanism of spin-order induced polarization in type-II multiferroics and guide the search for new materials for room-temperature applications, several theories have been built up. In 2005, Katsura, Nagaosa and Balatsky [24] proposed a microscopic pure electronic model (i.e., KNB model) combined with spin orbit coupling (SOC) and on site Coulomb repulsion to explain the polarization induced by the spiral spin structure. Then in 2006, Sergienko and Dagotto [25] attributed the polarization in $RMnO_3$ (R = Gd, Tb, Dy) to the

* Corresponding author.
E-mail address: hxiang@fudan.edu.cn (H.J. Xiang).

http://dx.doi.org/10.1016/j.commatsci.2015.08.041
0927-0256/

inverse DM interaction. Both models require the same conditions, namely, the SOC effect and noncollinear spin order. In the same year, Sergienko, Sen and Dagotto [26] showed that the E-type collinear magnetic order can also evoke ferroelectric polarization even without SOC. Later, Jia et al. [27] proposed a bond polarization model to explain the longitudinal polarization in the spin spiral system. Some phenomenological theories based on symmetry analysis have also been built to describe the coupling between spin order and ferroelectric polarization [28]. More recently, we [29–34] established a unified model for the microscopic mechanism of spin-order induced ferroelectricity in multiferroics, which includes the pure electronic, ion displacement and lattice deformation contributions. It should be noted that in type-I multiferroics, there may also exist spin-order induced polarization and the model is also applicable.

In this review, we first briefly introduce the previous models. Then our unified model will be discussed in detail.

2. Previous models for the spin-order induced ferroelectric polarization

In this part, we briefly review the previous models of the spin-order (both noncollinear and collinear) induced ferroelectric polarization.

2.1. Noncollinear spin structure induced electric polarization

There are various types of noncollinear magnetic structures, among which the two famous configurations are known as cycloidal spiral and proper screw spin structures (see Fig. 1b and c). In both cases the inversion symmetry is broken, where cycloidal spiral spin configuration often induces polarization and proper screw rarely produces polarization. In the following, we will introduce various models of noncollinear spin structures induced ferroelectric polarization.

2.1.1. KNB model

In 2005, Katsura, Nagaosa and Balatsky [24] proposed a microscopic model to explain the origin of electric polarization induced by noncollinear magnetic order. In their model, they first consider a three atoms cluster (i.e. two magnetic ions and the ligand oxygen ion) with inversion symmetry (Fig. 1(a)), and thus no DM interaction appears. The low-energy Hilbert space here is two dimensional with the basis generated from t_{2g} orbitals plus the on-site SOC effect. The Hamiltonian contains the on-site Coulomb repulsion of the magnetic ions and the hopping processes between the magnetic site and the oxygen site, and the hopping term is treated as perturbation. After a series of derivation, they obtain a concise result that the polarization direction is perpendicular to both the spin current direction and the vector connecting the magnetic ions. In both the double-exchange interaction and superexchange interaction cases, the polarization has the same form that $\vec{P} \cong A\vec{e}_{12} \times (\vec{e}_1 \times \vec{e}_2)$ (see Fig. 1(a)) where A is coefficient, $\vec{e}_{12}$ is the unit vector from site M1 to site M2 and $\vec{e}_1$ and $\vec{e}_2$ are the noncollinear spin directions. The spin current between M1 and M2 is described as $\vec{j}_s \propto \vec{e}_1 \times \vec{e}_2$.

With KNB model, one can easily find that the cycloidal spin structure (see Fig. 1(b)) induces a net polarization, while the proper screw spin structure (see Fig. 1(c)) gives no polarization. In 2003, Kimura et al. [19] found spontaneous polarization and strong magnetoelectric coupling in single crystal $TbMnO_3$ below 27 K. And in 2005, Kenzelmann et al. [35] established the magnetic structure of $TbMnO_3$ using neutron diffraction. They confirmed that the paraelectric, magnetically incommensurate phase (28–41 K) holds a sinusoidally modulated collinear magnetic order. In the ferroelectric phase (below 28 K), a noncollinear cycloidal spiral spin structure lies in the bc plane. Applying the KNB model to $TbMnO_3$, one can deduce a reasonable result that no polarization occurs in sinusoidally modulated collinear magnetic order and the direction of polarization induced by cycloidal spiral spin structure is along c axis which consists with experiment. Note that the cations and anions are fixed in the KNB model, and it is a pure electronic model. In Kimura and his coworkers' [19] experiment they found atomic displacements, which indicate KNB model cannot explain experiment completely. Moreover, polarization induced by proper screw spin configuration has also been observed in MnI_2 [36], $CuFeO_2$ [37,38] and $ACrO_2$ (A = Cu, Ag) [39], while KNB model predicts a zero polarization in these systems.

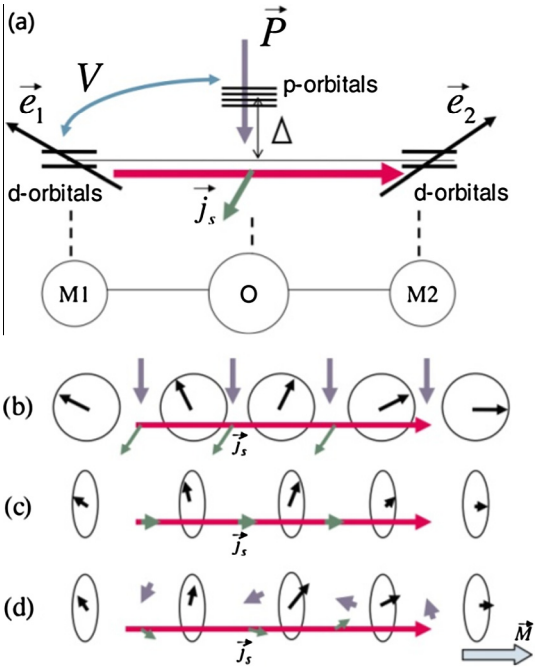

Fig. 1. (a) The cluster model with two transition metal ions M1, M2 with the oxygen atom O between them. The spin current $\vec{j}_s \propto \vec{e}_1 \times \vec{e}_2$ arises from the noncollinear spin direction $\vec{e}_1$ and $\vec{e}_2$. The direction of the electric polarization $\vec{P}$ is given by $\vec{P} \propto \vec{e}_{12} \times \vec{j}_S$ where $\vec{e}_{12}$ is the unit vector connecting M1 and M2. (b–d) Some of the specific configurations ((b): cycloidal spiral, (c): proper screw, (d): conical proper screw) where the geometrical relation among spins (black arrows), spin current (gray arrows), and electric polarization are shown [24]. © 2005, American Physical Society.

2.1.2. Inverse Dzyaloshinskii–Moryia (DM) interaction model

In order to explain the experiment that cycloidal spiral spin structure is accompanied by structural modulation in $TbMnO_3$, Sergienko and Dagotto [25] claimed that the noncollinear spin structure originates from DM interaction and its inverse interaction induces ferroelectric lattice displacement. DM interaction has the form: $\vec{D}_{ij} \cdot [\vec{S}_i \times \vec{S}_j]$, which was firstly proposed by Dzialoshinski [40] in 1958 to phenomenologically explain the weak ferromagnetism in α-Fe_2O_3. Then in 1960, Moriya [41] presented a microscopic picture by extending the theory of superexchange interaction to include the effect of SOC. In ferroelectric phase of $TbMnO_3$, it distorts from the cubic perovskite structure with the $GdFeO_3$-type cooperative rotation of the MnO_6 octahedra [42], where the bond angle of Mn–O–Mn deviates from 180° to about 145°. Adapting the symmetry analysis proposed by Moriya [41], the DM vector is nonzero with the direction perpendicular to the Mn–O–Mn bond plane. Sergienko and Dagotto [25] showed that the DM interaction linearly depends on the displacements of the O ions surrounding transition-metal ions. By minimizing the Hamiltonian containing the anisotropic exchange interaction and

the elastic energy with respect to the O ions displacements, one can get a global finite O ions displacement and a net ferroelectric polarization. Apparently, the inverse DM interaction model is a pure ionic displacement model in which only the oxygen ions can move and the cations are fixed.

Comparing the KNB model with the inverse DM interaction model, we can find that they require the same conditions, namely, SOC and spiral spin structure. They predict the same polarization direction, but through different ways (i.e., pure electronic and pure ionic, respectively). This is unsurprising that the Ginzburg–Landau approach [28] claims the form of the polarization is: $\vec{P} \propto \left(\vec{M}\cdot\nabla\right)\vec{M} - \vec{M}(\nabla\cdot\vec{M})$, which gives the same result as the KNB model and the inverse DM interaction model. In real materials, the electronic wave function deformation and ionic displacements always contribute to the total polarization simultaneously. This limits the application of the KNB model and the inverse DM interaction model to real materials. Both of the two models predict no polarization in collinear spin systems.

2.1.3. Bond polarization model

In proper screw spin configuration where the spin rotation plane is perpendicular to the spin propagation vector $\vec{q}$, both the KNB model and the inverse DM interaction model give a zero polarization. The representative systems are $CuFeO_2$ [37,38] and $ACrO_2$ (A = Cu, Ag) [39], whose magnetic structure is the helical spin spiral order with $\vec{q} = (Q, Q, 0)$, where $Q \approx 1/3$. Their polarization is parallel to $\vec{q}$. In 2007, Arima [43] claimed that the ferroelectric polarization in $CuFeO_2$ can be explained by the bond polarization model. The bond polarization model was proposed by Jia et al. [27] in 2006. They adopted the same M–O–M cluster model as that in KNB model. The difference between them is that bond polarization model contains a strong Hund coupling. They showed that there appears a longitudinal polarization P_x along the direction of the M–O–M cluster, which is roughly proportional to $(m_r^x)^2 - (m_l^x)^2$ where $m_{r(l)}^x$ is the x component of the spin orientation vector of the right (left) magnetic ion. The SOC effect is necessary in this model. By adopting this model, Arima suggested that the polarization in $CuFeO_2$ originates from the variation in the d-p hybridization with SOC, and the expression is $\vec{P}_{ij} \propto (\vec{S}_i\cdot\vec{e}_{ij})\vec{S}_i - (\vec{S}_j\cdot\vec{e}_{ij})\vec{S}_j$, where $\vec{e}_{ij}$ is the unit vector along the spin dimer. However in the case of $CuFeO_2$, the magnetic ion Fe^{3+} itself is an inversion center, and bond polarization model gives a zero total polarization, as we will show below.

Ba_2CoGeO_7 [44] shows tetragonal noncentrosymmetric structure with the space group $P\bar{4}2_1m$. There are two inequivalent Co sites in Ba_2CoGeO_7, but it is nonpolar in the paramagnetic phase. Below $T_N = 6.7$ K, their spins align in a collinear antiferromagnetic structure in the ab plane, and the ferroelectric polarization appears along the c axis even at $H = 0$. Through Landau phenomenological theory, first principles calculations and microscopic model derivation, Yamauchi et al. [45] showed that the ferroelectricity in Ba_2CoGeO_7 can be well explained by the bond polarization model, where the anisotropic p-d hybridization between Co and O states and the on-site SOC effect cause the local electric polarization.

2.2. Exchange striction model

Although the magnetoelectric coupling in noncollinear spin multiferroics is strong, the polarization is always small in these systems. This limits their realistic applications. The microscopic driving force of the polarization in the noncollinear spin multiferroics is SOC, which is not strong in the 3d transition metals, and leads to a small polarization. In 2006, Sergienko et al. [26] predicted ferroelectricity in orthorhombic perovskite $HoMnO_3$ induced by E-phase magnetic structure. In contrast to the case of spiral magnetic structure, the mechanism responsible for ferroelecticity in $HoMnO_3$ with the collinear magnetic structure has nothing to do with SOC. The Mn atoms with parallel spins form zigzag chains in the basal plane, and along the nearest neighbor Mn–Mn linear direction the magnetic order is of the type ↑↑↓↓ which obviously breaks the inversion symmetry. They attributed the polarization to the enhancement of the double exchange interaction, which induces a global oxygen ion displacement, that the bond angle of ferromagnetic Mn–O–Mn is larger than that of antiferromagnetic Mn–O–Mn. Sergienko et al. [26] claimed that the polarization of this type of multiferroic is two orders of magnitude larger than that in spiral magnets. Picozzi et al. [46] verified this prediction through first-principles calculations. The calculated polarization of the AFM-E phase $HoMnO_3$ is about 6 μC/cm^2, containing both ionic displacement and electronic deformation contributions. Lorenz et al. [47] observed the magnetic transition and the ferroelectric polarization in E-type phase of $HoMnO_3$ in experiment. Though the experimental magnitude of polarization is smaller than the predicted value, it is expected that the polarization will approach the theoretical value with the progress of the experimental technique and sample quality.

Another example that possesses exchange striction mechanism [$\vec{P}_{ij} \propto \left(\vec{S}_i\cdot\vec{S}_j\right)$] is Ca_3CoMnO_6 [48] discovered by Cheong's group. They measured the magnetic order of Ca_3CoMnO_6 by neutron diffraction to be up-up-down-down (↑↑↓↓) type. The Co^{2+} and Mn^{4+} ions alternate along the quasi-one-dimensional chains. This magnetic order (i.e. ↑↑↓↓) breaks the inversion symmetry and the exchange striction modulates the ferro(↑↑) and antiferro(↑↓) bond lengths leading to a global ferroelectricity. Through first principles calculations, Zhang et al. [49] confirmed that the ↑↑↓↓ spin order could indeed induce a ferroelectric polarization in Ca_3CoMnO_6. However, the magnitude of the predicted electric polarization is much greater than that in experiment. The discrepancy may be caused by the presence of different domains with opposite ferroelectric polarization in a single crystal. Through first principles calculations, Wang et al. [50] suggested that the spontaneous polarization in $TbMn_2O_5$ [21] could also be explained by the exchange striction model.

3. Unified model for the spin order induced improper ferroelectric polarization

The previous models give some reasonable explanations of the spin order induced improper ferroelectric polarization. However, there are also some problems to be addressed. They are either the pure electronic model (i.e., KNB model, bond polarization model) or the pure ionic displacement model (i.e. inverse DM interaction model, exchange stiction model). And some experimental results (such as ferroelectric polarization induced by proper screw spin order) could not be explained by previous models. Recently, we [29–34] develop a unified model for spin order induced improper ferroelectric polarization of multiferroics. This unified model can explain the polarization induced by any spin structures: collinear, cycloidal spiral, proper screw, etc. The total electric polarization $\vec{P}_t = \vec{P}_t(\vec{S}_1, \vec{S}_2, \ldots, \vec{S}_m; \vec{u}_1, \vec{u}_2, \ldots, \vec{u}_n; \eta_1, \eta_2, \ldots, \eta_6)$ of a magnetic system is a function of the spin direction $\vec{S}_i$ of the magnetic ion i, the displacement $\vec{u}_k$ of ion k and the homogeneous strain η_j. Here the spin order induced ion displacement $\vec{u}_k$ and the homogeneous strain η_j are given with respect to a reference structure (usually paraelectric structure). For simplicity, we use the notation $\vec{U} = (\vec{u}_1, \vec{u}_2, \ldots, \vec{u}_n)$ and $\Theta = (\eta_1, \eta_2, \ldots, \eta_6)$. Since the spin order induced ion displacement $\vec{u}_k$ and the strain η_j are rather small, the total FE polarization is estimated accurately by $\vec{P}_t \approx \vec{P}_e\left(\vec{S}_1, \vec{S}_2, \ldots, \vec{S}_m; \vec{U} = 0; \Theta = 0\right) + \vec{P}_{\text{ion,lattice}}\left(\vec{U}; \Theta\right)$, where

$\vec{P}_e$ is the pure electronic contribution and $\vec{P}_{\text{ion,lattice}}$ is the ion displacement and lattice deformation contributions (see Fig. 2). The pure electronic contribution arises from the electron density redistribution induced by the spin order. For the ion displacement part, it results from the ion displacement caused by the induced forces associated with the spin order. And the lattice-deformation contribution results from the spin order induced stress.

3.1. Pure electronic contribution of spin order induced polarization

3.1.1. Theoretical derivation

First, we will derivate the pure electronic contribution. Consider a spin dimmer in general case where the noncollinear spin arrangement breaks the inversion symmetry and leads to a polarization. Without loss of generality, we assume the distance vector from spin 1 to spin 2 is along the x axis. In general, the polarization is the function of spin 1 and spin 2, that is, $\vec{P} = \vec{P}(S_{1x}, S_{1y}, S_{1y}; S_{2x}, S_{2y}, S_{2z})$. The expression of $\vec{P}$ can be expanded as the Taylor series of $S_{i\alpha}(i = 1,2; \alpha = x,y,z)$. The electric polarization is an invariant under time reversal. Inverting the two spin directions simultaneously leave the electric polarization unchanged. The odd terms of the Taylor expansion should vanish due to the time reversal symmetry. If the fourth and higher order terms are neglected (confirmed by first principles calculations), the expression of $\vec{P}$ only contains the second order terms. And here we classify the polarization as intrasite $\vec{P}_i(\vec{S}_i)(i = 1,2)$ and intersite $\vec{P}_{12}(\vec{S}_1, \vec{S}_2)$ contributions. Then $\vec{P}$ can be written as

$$\vec{P} = \vec{P}_1\left(\vec{S}_1\right) + \vec{P}_2(\vec{S}_2) + \vec{P}_{12}(\vec{S}_1, \vec{S}_2), \quad \text{where}$$

$$\vec{P}_i(\vec{S}_i) = \sum_{\alpha\beta} \vec{P}_i^{\alpha\beta} S_{i\alpha} S_{i\beta}, \quad \text{and} \quad \vec{P}_{12}(\vec{S}_1, \vec{S}_2) = \sum_{\alpha\beta} \vec{P}_{12}^{\alpha\beta} S_{1\alpha} S_{2\beta}.$$

Here the coefficients $\vec{P}_i^{\alpha\beta}$ and $\vec{P}_{12}^{\alpha\beta}$ are vectors. Apparently, we can get the following relations: $\vec{P}_i^{\beta\alpha} = \vec{P}_i^{\alpha\beta}$, $\vec{P}_i(\vec{S}_i) = \vec{P}_i(-\vec{S}_i)$, $\vec{P}_{12}(-\vec{S}_1, \vec{S}_2) = \vec{P}_{12}(\vec{S}_1, -\vec{S}_2) = -\vec{P}_{12}(\vec{S}_1, \vec{S}_2)$. The intersite term can be written as:

$$\begin{aligned}
\vec{P}_{12}(\vec{S}_1, \vec{S}_2) &= \sum_{\alpha\beta} \vec{P}_{12}^{\alpha\beta} S_{1\alpha} S_{2\beta} \\
&= (S_{1x}, S_{1y}, S_{1z}) \begin{bmatrix} \vec{P}_{12}^{xx} & \vec{P}_{12}^{xy} & \vec{P}_{12}^{xz} \\ \vec{P}_{12}^{yx} & \vec{P}_{12}^{yy} & \vec{P}_{12}^{yz} \\ \vec{P}_{12}^{zx} & \vec{P}_{12}^{zy} & \vec{P}_{12}^{zz} \end{bmatrix} \begin{bmatrix} S_{2x} \\ S_{2y} \\ S_{2z} \end{bmatrix} \\
&= \vec{S}_1^T \vec{P}_{int} \vec{S}_2
\end{aligned}$$

As in the case of spin exchange interactions [51], $\vec{P}_{int}$ can be written as $\vec{P}_{int} = \vec{P}_J + \vec{P}_D + \vec{P}_\Gamma$, where $\vec{P}_J$, $\vec{P}_D$ and $\vec{P}_\Gamma$ are isotropic symmetric diagonal matrix, antisymmetric matrix and anisotropic symmetric matrix:

$$\vec{P}_J = \frac{1}{3} \begin{bmatrix} \vec{P}_{12}^{xx} + \vec{P}_{12}^{yy} + \vec{P}_{12}^{zz} & 0 & 0 \\ 0 & \vec{P}_{12}^{xx} + \vec{P}_{12}^{yy} + \vec{P}_{12}^{zz} & 0 \\ 0 & 0 & \vec{P}_{12}^{xx} + \vec{P}_{12}^{yy} + \vec{P}_{12}^{zz} \end{bmatrix}$$

$$\vec{P}_D = \frac{1}{2} \begin{bmatrix} 0 & \vec{P}_{12}^{xy} - \vec{P}_{12}^{yx} & \vec{P}_{12}^{xz} - \vec{P}_{12}^{zx} \\ \vec{P}_{12}^{yx} - \vec{P}_{12}^{xy} & 0 & \vec{P}_{12}^{yz} - \vec{P}_{12}^{zy} \\ \vec{P}_{12}^{zx} - \vec{P}_{12}^{xz} & \vec{P}_{12}^{zy} - \vec{P}_{12}^{yz} & 0 \end{bmatrix}$$

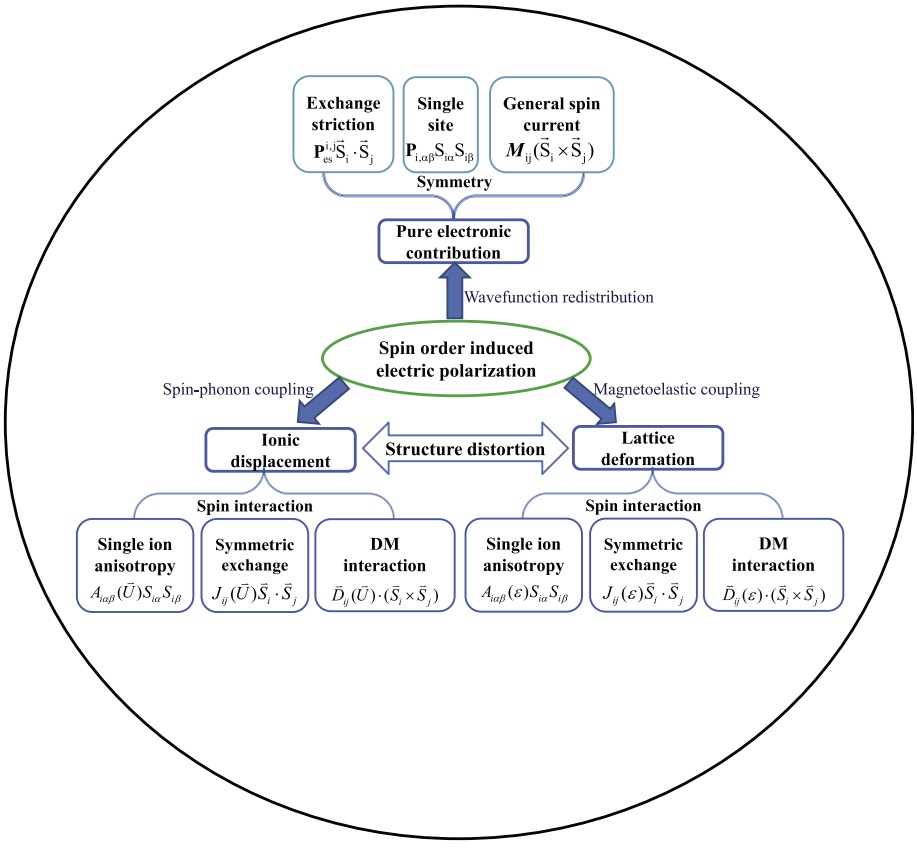

Fig. 2. Schematic illustration of three contributions to the electric polarization induced by a spin order in multiferroics [30].

$$\vec{P}_I = \begin{bmatrix} \vec{P}^{xx}_{12} - \frac{1}{3}(\vec{P}^{xx}_{12} + \vec{P}^{yy}_{12} + \vec{P}^{zz}_{12}) & \frac{1}{2}(\vec{P}^{xy}_{12} + \vec{P}^{yx}_{12}) & \frac{1}{2}(\vec{P}^{xz}_{12} + \vec{P}^{zx}_{12}) \\ \frac{1}{2}(\vec{P}^{yx}_{12} + \vec{P}^{xy}_{12}) & \vec{P}^{yy}_{12} - \frac{1}{3}(\vec{P}^{xx}_{12} + \vec{P}^{yy}_{12} + \vec{P}^{zz}_{12}) & \frac{1}{2}(\vec{P}^{yz}_{12} + \vec{P}^{zy}_{12}) \\ \frac{1}{2}(\vec{P}^{zx}_{12} + \vec{P}^{xz}_{12}) & \frac{1}{2}(\vec{P}^{zy}_{12} + \vec{P}^{yz}_{12}) & \vec{P}^{zz}_{12} - \frac{1}{3}(\vec{P}^{xx}_{12} + \vec{P}^{yy}_{12} + \vec{P}^{zz}_{12}) \end{bmatrix}.$$

In all known systems, the anisotropic symmetric term $\vec{P}_I$ is always small and can be neglected.

The general formula for the polarization of a spin dimer can be reduced in some special cases. First, we consider the case that the SOC effect is absent. The polarization of the system should not change under any global rotation of all the spins without SOC. In this case, the expression of the polarization can be drastically simplified. Now we show that $\vec{P}^{xx}_{12} = \vec{P}^{yy}_{12} = \vec{P}^{zz}_{12}$ without the SOC effect. Consider two spin arrangements:

Arrangement I : $\vec{S}_1 = (S_x, 0, 0); \vec{S}_2 = (0, S_y, 0)$

Arrangement II : $\vec{S}_1 = (S_x, 0, 0); \vec{S}_2 = (0, -S_y, 0).$

Arrangement II can be obtained by performing a spin rotation of arrangement I along the x axis by 180°. Therefore, $\vec{P}^{xy}_{12}$ should be zero because these two states have the same polarization without the SOC effect. Similarly, one can show that all the nondiagonal elements are zero. Now consider three spin arrangements that

Arrangement I : $\vec{S}_1 = (S_x, 0, 0); \vec{S}_2 = (S_x, 0, 0)$

Arrangement II : $\vec{S}_1 = (0, S_y, 0); \vec{S}_2 = (0, S_y, 0)$

Arrangement III : $\vec{S}_1 = (0, 0, S_z); \vec{S}_2 = (0, 0, S_z),$

where $S_x = S_y = S_z$. The three arrangements share the same polarization, because they are connected by the global rotations. Easily we can get $\vec{P}^{xx}_{12} = \vec{P}^{yy}_{12} = \vec{P}^{zz}_{12}$. Therefore, we can obtain the ordinary symmetric exchange striction term $\vec{P}_{12}(\vec{S}_1, \vec{S}_2) = \vec{P}_{es}(\vec{S}_1 \cdot \vec{S}_2)$, where $\vec{P}_{es} = \vec{P}^{xx}_{12} = \vec{P}^{yy}_{12} = \vec{P}^{zz}_{12}$.

Then let us consider a spin dimer with spatial inversion symmetry at the center. Combining the time reversal symmetry and the spatial inversion symmetry, we will show that $\vec{P}^{\alpha\beta}_1 = -\vec{P}^{\alpha\beta}_2$ and $\vec{P}^{\alpha\beta}_{12} = -\vec{P}^{\beta\alpha}_{12}$. Since all the coefficients should remain unchanged in different spin configurations, we can choose special spin arrangements to show the above two relations.

To prove $\vec{P}^{\alpha\beta}_1 = -\vec{P}^{\alpha\beta}_2$, we consider the following two spin arrangements of the spin dimer.

Arrangement I : $\vec{S}_1 = \vec{S}_2 = \vec{S} = (S_x, S_y, S_z)$

Arrangement II : $\vec{S}_1 = -\vec{S}_2 = \vec{S} = (S_x, S_y, S_z).$

By applying spatial inversion symmetry and $\vec{S}_1 = \vec{S}_2$, we can obtain the relations that $\vec{P}_I(\vec{S}_1, \vec{S}_2) = -\vec{P}_I(\vec{S}_2, \vec{S}_1)$ and $\vec{P}_I(\vec{S}_1, \vec{S}_2) = -\vec{P}_I(\vec{S}_1, \vec{S}_2)$, that is $\vec{P}_I(\vec{S}_1, \vec{S}_2) = 0$. Similarly, we can get $\vec{P}_{II}(\vec{S}_1, \vec{S}_2) = -\vec{P}_{II}(-\vec{S}_1, -\vec{S}_2)$ under spatial inversion symmetry. Under time reversal symmetry, we can obtain the relation that $\vec{P}_{II}(\vec{S}_1, \vec{S}_2) = \vec{P}_{II}(-\vec{S}_1, -\vec{S}_2)$. Finally we will get $\vec{P}_{II}(\vec{S}_1, \vec{S}_2) = -\vec{P}_{II}(\vec{S}_1, \vec{S}_2) = 0$. The two arrangements I and II provide opposite contributions to the intersite polarization $\vec{P}_{12}$. Therefore, the sum $\vec{P}_{sum}$ of the electric polarizations of these two spin arrangements only contains the intrasite contributions.

$$\vec{P}_{sum} = 2\vec{P}_1(\vec{S}_1) + 2\vec{P}_2(\vec{S}_2) = 2\sum_{\alpha\beta}\left(\vec{P}^{\alpha\beta}_1 + \vec{P}^{\alpha\beta}_2\right)S_\alpha S_\beta.$$

Since $\vec{P}_I = \vec{P}_{II} = 0$, then $\vec{P}_{sum}$ should also be zero. Since $\vec{S}$ is arbitrary, we finally obtain the relation $\vec{P}^{\alpha\beta}_1 = -\vec{P}^{\alpha\beta}_2$.

Similarly, to prove that $\vec{P}^{\alpha\beta}_{12} = -\vec{P}^{\beta\alpha}_{12}$, we can also construct two spin arrangements with spatial inversion symmetry:

Arrangement I : $\vec{S}_1 = \vec{S}$ and $\vec{S}_2 = \vec{S}'$

Arrangement II : $\vec{S}_1 = \vec{S}'$ and $\vec{S}_2 = \vec{S}.$

The intersite term of the polarizations for these two spin arrangements is opposite, that is,

$$\sum_{\alpha\beta}\vec{P}^{\alpha\beta}_{12}S_\alpha S'_\beta = -\sum_{\alpha\beta}\vec{P}^{\alpha\beta}_{12}S'_\alpha S_\beta = -\sum_{\alpha\beta}\vec{P}^{\beta\alpha}_{12}S'_\beta S_\alpha.$$

The above equation shows that $\vec{P}^{\alpha\beta}_{12} = -\vec{P}^{\beta\alpha}_{12}$, and hence $\vec{P}^{\alpha\alpha}_{12} = 0$. With these relations we can reduce the intersite polarization as:

$$\begin{aligned}\vec{P}_{12}(\vec{S}_1, \vec{S}_2) &= \sum_{\alpha\beta}\vec{P}^{\alpha\beta}_{12}S_{1\alpha}S_{2\beta} \\ &= \vec{P}^{yz}_{12}(\vec{S}_1 \times \vec{S}_2)_x + \vec{P}^{zx}_{12}(\vec{S}_1 \times \vec{S}_2)_y \\ &\quad + \vec{P}^{xy}_{12}(\vec{S}_1 \times \vec{S}_2)_z,\end{aligned}$$

where $(\vec{S}_1 \times \vec{S}_2)_\alpha$ refers to the $\alpha(= x, y, z)$ component of the vector $\vec{S}_1 \times \vec{S}_2$. Now we can rewrite the intersite polarization to be $\vec{P}_{12} = \vec{M}(\vec{S}_1 \times \vec{S}_2)$ with the 3×3 matrix $\vec{M}$:

$$\vec{M} = \begin{bmatrix} (\vec{P}^{yz}_{12})_x & (\vec{P}^{zx}_{12})_x & (\vec{P}^{xy}_{12})_x \\ (\vec{P}^{yz}_{12})_y & (\vec{P}^{zx}_{12})_y & (\vec{P}^{xy}_{12})_z \\ (\vec{P}^{yz}_{12})_z & (\vec{P}^{zx}_{12})_z & (\vec{P}^{xy}_{12})_z \end{bmatrix}.$$

And the total electronic polarization of the noncollinear spin dimer with spatial inversion symmetry is

$$\vec{P} = \sum_{\alpha\beta}\vec{P}^{\alpha\beta}_1(S_{1\alpha}S_{1\beta} - S_{2\alpha}S_{2\beta}) + \vec{M}(\vec{S}_1 \times \vec{S}_2).$$

Now we compare this model to the previous pure electronic polarization models (i.e. KNB model [24] and bond polarization model [27]). Without loss of generality, we define the distance vector from spin 1 to spin 2 is taken along the x axis. If we set the $\vec{M}$ matrix to be $\vec{M} = \begin{bmatrix} 0 & 0 & 0 \\ 0 & 0 & -C \\ 0 & C & 0 \end{bmatrix}$, then the intersite term will become to $\vec{P}_{inter} = \vec{M}(\vec{S}_1 \times \vec{S}_2) = C\begin{bmatrix} 0 \\ -(\vec{S}_1 \times \vec{S}_2)_z \\ (\vec{S}_1 \times \vec{S}_2)_y \end{bmatrix} = C\vec{e}_{12} \times (\vec{S}_1 \times \vec{S}_2)$, and this is the KNB model. Thus KNB model is a special case of the intersite polarization with $(\vec{P}^{zx}_{12})_z = -(\vec{P}^{xy}_{12})_y = C$. The intersite term $\vec{M}(\vec{S}_1 \times \vec{S}_2)$ can be referred to as the generalized KNB (gKNB) model. The bond polarization model can be obtained by setting $\vec{P}^{xx}_1 = (C, 0, 0)$, $\vec{P}^{xy}_1 = \vec{P}^{yx}_1 = (0, C/2, 0)$, and $\vec{P}^{zx}_1 = \vec{P}^{xz}_1 = (0, 0, C/2)$. Then the intrasite polarization becomes to $\vec{P}_{intra} = \sum_{\alpha\beta}\vec{P}^{\alpha\beta}_1(S_{1\alpha}S_{1\beta} - S_{2\alpha}S_{2\beta}) = C\begin{bmatrix} S_{1x}S_{1x} - S_{2x}S_{2x} \\ S_{1x}S_{1y} - S_{2x}S_{2y} \\ S_{1x}S_{1z} - S_{2x}S_{2z} \end{bmatrix} = C\left[(\vec{S}_1 \cdot \vec{e}_{12})\vec{S}_1 - (\vec{S}_2 \cdot \vec{e}_{12})\vec{S}_2\right]$, where $\vec{e}_{12}$ is the unit vector along the x axis. The bond polarization model is a special case of the intrasite term of the total electronic polarization. We notice that the KNB model and the bond polarization are both derived from the three-atom linear M–O–M cluster model, and they are special cases of our general model.

When the magnetic ion itself is a spatial inversion center, the single site term will vanish. By applying the spatial inversion

symmetry, we can obtain the relation $\overrightarrow{P}_i(\overrightarrow{S}_i) = -\overrightarrow{P}_i(\overrightarrow{S}_i)$, that is $\overrightarrow{P}_i(\overrightarrow{S}_i) = 0$. Since $\overrightarrow{S}_i$ is arbitrary, the coefficients $\overrightarrow{P}_{i,\alpha\beta}$ should be zero. This suggests that the electric polarization induced by the spin order in $CuFeO_2$ cannot be explained by the bond polarization model as commonly believed in the literature.

In general, we can reformulate the spin order induced electronic contributions to the total polarization as: $\overrightarrow{P}_e = \sum_{i,\alpha\beta} \overrightarrow{P}_{i,\alpha\beta} S_{i\alpha} S_{i\beta} + \sum_{\langle i,j\rangle} \overrightarrow{P}^{ij}_{es} \vec{s}_i \cdot \vec{s}_j + \sum_{\langle i,j\rangle} \overrightarrow{M}^{ij}(\vec{s}_i \times \vec{s}_j)$, where $\overrightarrow{P}_{i,\alpha\beta}$, $\overrightarrow{P}^{ij}_{es}$ and $\overrightarrow{M}^{ij}$ are the coefficients of the single-site term, exchange striction term and general spin current term, respectively. Note that the anisotropic symmetric term $\overrightarrow{P}_I$ is neglected. The single-site term and the general spin current term are SOC related, while the exchange striction term does not depend on SOC. In magnetic multiferroics, the spin order induced ion displacements are rather small (usually $\ll$ 0.01 Å), so the electronic contribution remains almost unchanged after ion displacements. And we can choose a reference structure (usually a paraelectric (PE) centrosymmetric structure, but it also works for a proper FE case) to calculate the pure electronic contribution. The single site term $\overrightarrow{P}_{i,\alpha\beta}$ is usually small, but it is responsible for the ferroelectricity in Cu_2OSeO_3 [32]. In $CaMn_7O_{12}$ [34] the exchange striction term governs the magnitude of the polarization. The general spin current term can well explain the mechanism of the polarization in the helical magnetic order in MnI_2 system [33].

3.1.2. Determine coefficients for the pure electronic contributions

To calculate the polarizations of the general model, one needs to determine the expansion coefficients $\overrightarrow{P}_{i,\alpha\beta}$, $\overrightarrow{P}^{ij}_{es}$ and $\overrightarrow{M}^{ij}$. We proposed the so-called "four-states mapping" method to compute these expansion coefficients, in which the polarizations are calculated for a set of carefully chosen four spin arrangements. One can use substitution method to calculate the expansion coefficients for a given spin dimer, in which the magnetic ions other than the studied dimer are substituted with nonmagnetic ions. But this method is less accurate.

We show how to compute $\overrightarrow{P}^{yz}_{ij}$ of the $\overrightarrow{M}$ matrix as an example and the other coefficients can be extracted similarly (see Appendix A). Combined with the SOC effect, we calculate the electric polarizations of the following four spin arrangements for a spin dimer $\overrightarrow{S}_i$ and $\overrightarrow{S}_j$:

$$\begin{aligned}
&\text{I}: \ \overrightarrow{S}_i = (0,1,0); \quad \overrightarrow{S}_j = (0,0,1)\\
&\text{II}: \ \overrightarrow{S}_i = (0,1,0); \quad \overrightarrow{S}_j = (0,0,-1)\\
&\text{III}: \ \overrightarrow{S}_i = (0,-1,0); \quad \overrightarrow{S}_j = (0,0,1)\\
&\text{IV}: \ \overrightarrow{S}_i = (0,-1,0); \quad \overrightarrow{S}_j = (0,0,-1).
\end{aligned}$$

The other spins are set according to the experimental spin configuration and remain unchanged during the four calculations. The formula of the coefficient $\overrightarrow{P}^{yz}_{ij}$ can be expressed as $\overrightarrow{P}^{yz}_{ij} = \frac{\overrightarrow{P}^{I}_{+} \overrightarrow{P}^{IV}_{-} \overrightarrow{P}^{II}_{-} \overrightarrow{P}^{III}}{4}$. This procedure is similar to the "four-states mapping" method we proposed before to extract the DM interaction parameters of a magnetic system [29,52].

3.2. Ion displacement and lattice deformation contributions for spin order induced polarization

3.2.1. Theoretical derivation

In the previous section, we focus on the pure electronic contributions. Here, we will discuss how a spin order influences the ion displacement and lattice deformation, and subsequently induces a ferroelectric polarization. The ion displacement contribution to the polarization is obvious. The spin order induced lattice strain can give rise to an additional electric polarization through the piezoelectric effect [53,54]. For dielectric magnetic materials, the response properties can be systematically revealed through the electric–magnetic enthalpy as a function of ion displacement, strain, extra magnetic and electric field. In general, the total energy of a magnetic system can be written as $E(u_m, \eta_j, \overrightarrow{S}_i) = E_{PM}(u_m, \eta_j) + E_{spin}(u_m, \eta_j, \overrightarrow{S}_i)$, where u_m is the ion displacement of reference structure for all the ions, η_j is the homogeneous strain in Voigt notation, and $\overrightarrow{S}_i$ is the spin vector of all the magnetic ions. $E_{PM}(u_m, \eta_j)$ is the energy of the paramagnetic state with the form [53,55]:

$$E_{PM} = E_0 + \sum_m A_m u_m + \sum_j A_j \eta_j + \frac{1}{2}\sum_{m,n} B_{mn} u_m u_n + \frac{1}{2}\sum_{j,k} B_{jk}\eta_j\eta_k + \sum_{m,j} B_{mj} u_m \eta_j + \textit{terms of third and higher orders}.$$

The first order coefficients A_m and A_j refer to the force and stress, respectively. And the second order coefficients B_{mn}, B_{jk} and B_{mj} represent the force constant, frozen-ion elastic constant, and internal displacement tensor, respectively. Here the reference structure is in equilibrium in the paramagnetic state, that is, $\frac{\partial E_{PM}}{\partial u_m} = \frac{\partial E_{PM}}{\partial \eta_j} = 0$. Then we have $A_m = A_j = 0$.

The spin interaction energy E_{spin} can be expanded as $E_{spin} = E_H + E_{DM} + E_{SIA}$, where E_H is the Heisenberg symmetric exchange interaction energy, E_{DM} is the Dzyaloshinskii–Moriya (DM) interaction energy and E_{SIA} is the single-ion anisotropy energy. E_H, E_{DM} and E_{SIA} are the function of the ion displacement u_m, homogeneous strain η_j and the spin vector $\overrightarrow{S}_i$. We can express the Heisenberg symmetric interaction energy as $E_H = \sum_{i,i'} J^0_{i,i'} \overrightarrow{S}_i \cdot \overrightarrow{S}_{i'} + \sum_{i,i'} \frac{\partial J_{i,i'}}{\partial u_m} \overrightarrow{S}_i \cdot \overrightarrow{S}_{i'} u_m + \sum_{i,i'} \frac{\partial J_{i,i'}}{\partial \eta_j} \overrightarrow{S}_i \cdot \overrightarrow{S}_{i'} \eta_j + \sum_{i,i'} \frac{\partial^2 J_{i,i'}}{\partial u_m u_n} \overrightarrow{S}_i \cdot \overrightarrow{S}_{i'} u_m u_n + \sum_{i,i'} \frac{\partial^2 J_{i,i'}}{\partial \eta_j \eta_k} \overrightarrow{S}_i \cdot \overrightarrow{S}_{i'} \eta_j \eta_k + \sum_{i,i'} \frac{\partial^2 J_{i,i'}}{\partial u_m \eta_j} \overrightarrow{S}_i \cdot \overrightarrow{S}_{i'} u_m \eta_j +$ *terms of third and higher orders*. Here $J^0_{i,i'}$ is the Heisenberg symmetric exchange interaction parameter with $u_m = \eta_j = 0$, and $\frac{\partial J_{i,i'}}{\partial u_m}$, $\frac{\partial J_{i,i'}}{\partial \eta_j}$, $\frac{\partial^2 J_{i,i'}}{\partial u_m u_n}$, $\frac{\partial^2 J_{i,i'}}{\partial \eta_j \eta_k}$, and $\frac{\partial^2 J_{i,i'}}{\partial u_m \eta_j}$ are the derivatives of the exchange parameters. Similarly, the DM interaction energy E_{DM} and the single ion anisotropy energy E_{SIA} can also be expressed as the Taylor expansion of u_m and η_j. E_{DM} and E_{SIA} originate from the SOC effect and always one order smaller than the symmetric exchange interaction energy E_H. Usually, we only consider the E_H term.

Note that we use the implied-sum notation for m, n, j and k in the expression of E_H. The ion displacement and lattice deformation caused by the spin order can be obtained by minimizing the total energy $E(u_m, \eta_j, \overrightarrow{S}_i)$ with respect to u_m and η_j, that is,

$$\begin{cases} \frac{\partial E(u_m, \eta_j, \overrightarrow{S}_i)}{\partial u_m} = 0, \\ \frac{\partial E(u_m, \eta_j, \overrightarrow{S}_i)}{\partial \eta_j} = 0. \end{cases}$$

Then we can get $B_{mn} u_n + B_{mj}\eta_j = -\frac{\partial E_H}{\partial u_m}$, where $\frac{\partial E_H}{\partial u_m} = \sum_{i,i'} \frac{\partial J_{i,i'}}{\partial u_m} \overrightarrow{S}_i \cdot \overrightarrow{S}_{i'} - \sum_{i,i'} \frac{\partial^2 J_{i,i'}}{\partial u_m u_n} \overrightarrow{S}_i \cdot \overrightarrow{S}_{i'} u_n - \sum_{i,i'} \frac{\partial^2 J_{i,i'}}{\partial u_m \eta_j} \overrightarrow{S}_i \cdot \overrightarrow{S}_{i'} \eta_j$. Since $\frac{\partial^2 J_{i,i'}}{\partial u_m u_n} \ll B_{mn}$, $\frac{\partial^2 J_{i,i'}}{\partial u_m \eta_j} \ll B_{mj}$, we finally obtain

$$B_{mn} u_n + B_{mj}\eta_j = -\sum_{i,i'} \frac{\partial J_{i,i'}}{\partial u_m} \overrightarrow{S}_i \cdot \overrightarrow{S}_{i'},$$

$$B_{jk}\eta_k + B_{mj} u_m = -\sum_{i,i'} \frac{\partial J_{i,i'}}{\partial \eta_j} \overrightarrow{S}_i \cdot \overrightarrow{S}_{i'}.$$

The ion displacement u_m and strain η_j can be obtained by solving the above two linear equations. If the system in the PM state is piezoelectric, the lattice deformation induced by spin order may give rise to an additional electric polarization. The combined effect of spin order induced stress and piezoelectricity in piezoelectric crystal classes in PM state induces a lattice deformation contribution to the electric polarization. And the polarization induced by the ion displacement u_m and strain η_j can also be computed as $P_\alpha = Z_{\alpha m}u_m + e_{\alpha j}\eta_j$, where $Z_{\alpha m}$ and $e_{\alpha j}$ are the Born effective charge and frozen-ion piezoelectric tensor, respectively.

Note that both the ion displacement and lattice deformation contributions are included in P_α. If we want to obtain the polarization contribution due to the stress induced by spin order, we can set $-\sum_{i,i'}\frac{\partial J_{i,i'}}{\partial u_m}\vec{S}_i\cdot\vec{S}_{i'}=0$. And the corresponding polarization can be obtained by $P_\alpha = d_{\alpha j}\sigma_j$, where $\sigma_j = -\sum_{i,i'}\frac{\partial J_{i,i'}}{\partial \eta_j}\vec{S}_i\cdot\vec{S}_{i'}$ is the total stress due to the spin order. We can get $d_{\alpha j}$ by using $d_{\alpha j} = S_{jk}e_{\alpha k}$, where S_{jk} and $e_{\alpha k}$ are the relaxed-ion elastic compliance tensor and the relaxed-ion piezoelectric tensor, respectively.

3.2.2. Determine parameters of the model

Similar to the case of the pure electronic contribution, one can also obtain the parameters of ion displacement and lattice deformation contributions of the polarization. The Born effective charges $Z_{\alpha m}$, frozen-ion piezoelectric tensor $e_{\alpha j}$, force constant B_{mn} and the internal-displacement tensor B_{mj} can be obtained by the density functional perturbation theory (DFPT). And the frozen-ion elastic constant B_{jk} can be easily obtained by calculating strain–stress relation within DFT. In principle, these parameters are preferred to be obtained in the PM state. To a first approximation, those obtained from the FM state are sufficient, which are readily determined using the DFPT.

For the parameters $\frac{\partial J_{i,i'}}{\partial u_m}$, and $\frac{\partial J_{i,i'}}{\partial \eta_j}$, we can also use the four-states mapping method [31,52], where $\frac{\partial J_{i,i'}}{\partial u_m}$ and $\frac{\partial J_{i,i'}}{\partial \eta_j}$ are calculated without SOC. We consider the following four spin states for site i and i':

$$\text{I}: \ \vec{S}_i = (0,0,1); \quad \vec{S}_{i'} = (0,0,1)$$

$$\text{II}: \ \vec{S}_i = (0,0,1); \quad \vec{S}_{i'} = (0,0,-1)$$

$$\text{III}: \ \vec{S}_i = (0,0,-1); \quad \vec{S}_{i'} = (0,0,1)$$

$$\text{IV}: \ \vec{S}_i = (0,0,-1); \quad \vec{S}_{i'} = (0,0,-1)$$

The other spins are set according to the experimental spin configuration and remain unchanged during the four calculations. The paramters can be easily obtained that: $\frac{\partial J_{i,i'}}{\partial u_m} = \frac{1}{4}\left(\frac{\partial E_{\text{I}}}{\partial u_m} + \frac{\partial E_{\text{IV}}}{\partial u_m} - \frac{\partial E_{\text{II}}}{\partial u_m} - \frac{\partial E_{\text{III}}}{\partial u_m}\right)$ and $\frac{\partial J_{i,i'}}{\partial \eta_j} = \frac{1}{4}\left(\frac{\partial E_{\text{I}}}{\partial \eta_j} + \frac{\partial E_{\text{IV}}}{\partial \eta_j} - \frac{\partial E_{\text{II}}}{\partial \eta_j} - \frac{\partial E_{\text{III}}}{\partial \eta_j}\right) = -\frac{1}{4}(\sigma_j^{\text{I}} + \sigma_j^{\text{IV}} - \sigma_j^{\text{II}} - \sigma_j^{\text{III}})$.

4. Applications of the unified model of spin order induced ferroelectric polarization

The three parts of pure electronic polarization vary in different materials. In Cu_2OSeO_3 [32], in which the magnetoelectric Skymions have been observed, the single site term contributes its polarization. While in $CaMn_7O_{12}$ [34], the direction of the electric polarization is determined by the chirality of the helical magnetic order due to the DM interaction, and its magnitude is governed by the exchange striction. The polarization induced by the helical spin order in MnI_2 [33] can be well explained by the general spin current term. In $BiFeO_3$ [30], the pure electronic, ion displacement, and lattice deformation contributions are of comparable magnitude.

4.1. Combined effect of exchange striction and DM interaction in $CaMn_7O_{12}$

$CaMn_7O_{12}$ [22,23] is a recent discovered multiferroic. Below ~440 K, it is transformed into a phase with the structure adopting the space group $R\bar{3}$, in which there are one Mn^{4+} (Mn3) and six Mn^{3+} per formula unit (FU). The neutron diffraction measurements show that in the temperature range of 48–90 K, $CaMn_7O_{12}$ adopts a helical magnetic state with propagation vector $(0, 1, 0.963)$. More interestingly, it also exhibits a giant improper ferroelectric polarization ($2870\ \mu C/m^2$) along the c direction after the onset of the helical magnetic order at 90 K. To gain insights into the origin of this giant improper polarization, we apply our unified model to this system [34]. We first examine the ferroelectric polarization of $CaMn_7O_{12}$ by using the experimental helical magnetic state with the commensurate propagation vector $(0, 1, 1)$. Our results show that the ferroelectric polarization is along the c direction with $P_z = 4496\ \mu C/m^2$ from DFT + U + SOC calculations, but $P_z = 3976\ \mu C/m^2$ from DFT + U calculations. Thus, the giant improper ferroelectric polarization in $CaMn_7O_{12}$ is mainly caused by the exchange striction rather than by SOC since the spin dimers of $CaMn_7O_{12}$ are noncentrosymmetric. According to our unified model, for a spin dimer containing two spin sites 1 and 2 with no inversion symmetry at the center, the polarization $\vec{P}_{12}$ induced by the spin arrangement $(\vec{S}_1, \vec{S}_2)$ in the absence of SOC effect can be written as the usual symmetric exchange striction term $\vec{P}_{12}(\vec{S}_1, \vec{S}_2) = \vec{P}_{es}(\vec{S}_1\cdot\vec{S}_2)$. If the distance between the magnetic ions in a spin dimer is restricted to be shorter than 3.7 Å, there are seven different spin exchange paths J_1–J_7 between the $Mn1^{3+}$, $Mn2^{3+}$ and $Mn3^{4+}$ ions. For the seven exchange paths of the experimental $CaMn_7O_{12}$ structure, we evaluate their $\vec{P}_{es}$ by performing DFT + U calculations using the "four-states mapping" method similar to that used to extract the spin exchange parameters. Our calculations show that two exchange paths J_4 and J_5 have the largest coefficients, that is, $\vec{P}^4_{es} = (-0.024, -0.042, 0.029)$eÅ and $\vec{P}^5_{es} = (-0.026, -0.048, 0.054)$eÅ. The remaining spin exchange paths have much smaller coefficients. The contribution of $\vec{P}^5_{es}$ to the total electric polarization vanishes by symmetry, but $\vec{P}^4_{es}$ has a large contribution to the total electric polarization. Because of the threefold rotational symmetry, the total polarization is along z axis. The polarization per $Mn3^{4+}$ from the exchange striction mechanism can be written as

$$\begin{aligned} P_z &= P^z_{es,4}\left[\vec{S}_0\cdot(\vec{S}_1 - \vec{S}_4 + \vec{S}_2 - \vec{S}_5 + \vec{S}_3 - \vec{S}_6)\right] \\ &= 3P^z_{es,4}\,\vec{S}_0\cdot(\vec{S}_1 - \vec{S}_4) \\ &= 3P^z_{es,4}|\vec{S}_4 - \vec{S}_1|\left[(\cos\alpha)\vec{e}_x + (\sin\alpha)\vec{e}_y\right]\cdot\vec{e}_y \text{sign}\left[\vec{e}_z\cdot(\vec{S}_4\times\vec{S}_1)\right] \\ &= 3\sqrt{3}P^z_{es,4}(\sin\alpha)\text{sign}\left[\vec{e}_z\cdot(\vec{S}_4\times\vec{S}_1)\right], \end{aligned}$$

where we set $|\vec{S}_i| = 1$, and define the unit vector $\vec{e}_x$ along the direction of $\vec{S}_1 + \vec{S}_4$, and $\vec{e}_y$ orthogonal to $\vec{e}_x$ in the plane as in Fig. 3(a) so that $\vec{e}_z = \vec{e}_x\times\vec{e}_y$ points toward the readers. Thus if $\vec{S}_1\times\vec{S}_4$ is along $\vec{e}_z$, then $\vec{S}_4 - \vec{S}_1$ is along $\vec{e}_y$, i.e., $\frac{\vec{S}_1 - \vec{S}_4}{|\vec{S}_1 - \vec{S}_4|} = \vec{e}_y\text{sign}\left[\vec{e}_z\cdot(\vec{S}_4\times\vec{S}_1)\right]$. The spins of the two different sets make the angle of 120° between them. Given α as the angle the spin vector $\vec{S}_0$ makes with $\vec{e}_x$. Thus the magnitude of P_z depends almost linearly on α, since $\sin\alpha \approx \alpha$ for

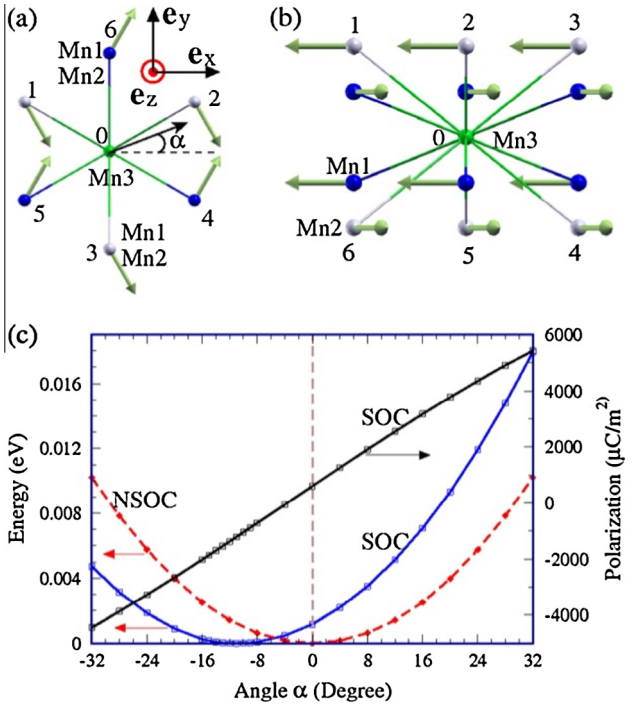

Fig. 3. (a, b) The top and side views of six $Mn1^{3+}$ and six $Mn2^{3+}$ ions surrounding a $Mn3^{4+}$ ion. (c) The total energy and electric polarization as a function of the $Mn3^{4+}$ spin direction α [34]. © 2012 American Physical Society.

small α [see Fig. 3(c)]. This result is consistent with the direct DFT calculations. When $\alpha = -30°$, the polarization becomes $-4000\ \mu C/m^2$. It should be noted that α indicates the orientation of $Mn3^{4+}$, which is determined by the strong DM interaction in J_4 path. Therefore, the large improper electric polarization in $CaMn_7O_{12}$ originates from the combined effect of the exchange striction and DM interaction. Moreover, it can be found from the above equation that the direction of the polarization depends on the scalar chirality of the helical magnetic structure $\sigma \propto \vec{e}_z \cdot (\vec{S}_4 \times \vec{S}_1) \propto \vec{r}_{41} \cdot (\vec{S}_4 \times \vec{S}_1)$.

4.2. General spin current induced ferroelectric polarization in triangular-lattice antiferromagnets

The layered iodide MnI_2 [36], which crystallizes in the CdI_2 type structure with centrosymmetric space group $P\bar{3}m1$, exhibits ferroelectricity under external magnetic field with the helical spin-spiral order below phase transition temperature 3.45 K. The magnetic ground state of MnI_2 is proper screw, where spins rotate within the plane perpendicular to the magnetic modulation vector $\vec{k} \sim (0.181, 0, 0.439)$, and no polarization occurs in zero external magnetic field. The in-plane component $\vec{q}$ of the $\vec{k}$ vector dominates the ME properties of MnI_2 as demonstrated in experiment, and the spins favor to lie within the plane perpendicular to the applied magnetic field H. Under a low in-plane magnetic field ($H < 3T$), the proper screw spin order adopts the in-plane component $\vec{q} \| \langle 1\bar{1}0 \rangle$, with the polarization $\vec{P} \| \langle 110 \rangle \perp \vec{q}$. When the external in-plane magnetic field is in the range of 3T–7T, the polarization $\vec{P}$ is parallel to $\vec{q} \| \langle 110 \rangle$. In both cases the polarization can flop when rotating the applied H along the [001] direction, indicting strong ME coupling in this system.

We adopt the unified model to explain the polarization of MnI_2 [33]. Note that there exists spatial inversion symmetry at the center of the Mn-Mn spin dimer, and the diagonal coefficients of the intersite polarization vanish. Using the "four-states mapping" method, one can readily determine the expansion coefficients $\vec{P}_i^{\alpha\beta}$ and $\vec{M}$ matrix for a given spin dimer. The coefficients of the intrasite polarization are indeed negligible, for the fact that Mn^{2+} ion itself is an inversion center. The $\vec{M}$ matrix of the intersite polarization are calculated as $\vec{M} = \begin{bmatrix} -4.8 & 0 & 0 \\ 0 & 39.5 & 49.0 \\ 0 & -44.5 & -26.0 \end{bmatrix}$, in units of 10^{-5} eÅ. This differs from the KNB model because the matrix elements $M_{11} = (\vec{P}_{12}^{yz})_x$, $M_{22} = (\vec{P}_{12}^{zx})_y$ and $M_{33} = (\vec{P}_{12}^{xy})_z$ are not zero and $M_{23} = (\vec{P}_{12}^{xy})_y \neq -M_{32} = (\vec{P}_{12}^{zx})_z$. Fig. 4(c) shows the differences between the KNB and gKNB models in predicting the polarization $\vec{P}$. Fig. 4(d) shows the polarization predicted by gKNB model is in good agreement with the value directly calculated from the density functional calculations for the given spin dimer.

We now compare the total ferroelectric polarization of MnI_2 extracted by the gKNB model and direct density functional calculations. In the helical spin-spiral order, the sum of the intrasite polarization is zero, and the intersite polarization for site i is $\vec{P}_i^{tot} = \sum_{k=1}^{6} \vec{P}_{ik}$, which is the same for all i sites. So the total polarization for site 0, shown in Fig. 4(b), is $\vec{P}_0^{tot} = \sum_{k=1}^{6} \vec{P}_{0k} = \sum_{k=1}^{6} \vec{M}^{0k}(\vec{S}_0 \times \vec{S}_k)$. For $\vec{q} = (Q, 0, 0)$, $\vec{P}_0^{tot} = \left(\frac{\sqrt{3}}{2}A, -\frac{3}{2}A, 0\right)$ with $A = (M_{11} - M_{22})\sin 2\pi Q$. In the case of $\vec{q} = (Q, Q, 0)$, $\vec{P}_0^{tot} = \left(\frac{1}{2}B, \frac{\sqrt{3}}{2}B, 0\right)$ with $B = (M_{11} + 3M_{22} - 4M_{11}\cos 2\pi Q)\sin 2\pi Q$. Thus the gKNB model predicts that $\vec{P} \perp \vec{q}$ in the low applied field that $\vec{q} = (Q, 0, 0)$, but $\vec{P} \| \vec{q}$ in the high applied field that $\vec{q} = (Q, Q, 0)$, which is consistent with the experiment. And the polarization reverses when changing the spin chirality from right to left (i.e. $\vec{q}$ to $-\vec{q}$), also in accord with the experiment. By setting $Q = 1/3$, the density functional calculations show that the electronic polarization of $\vec{q} = (Q, 0, 0)$ is 58.8 $\mu C/m^2$ along the $[0\bar{1}0]$ direction, and in the case of $\vec{q} = (Q, Q, 0)$, the polarization is 71.4 $\mu C/m^2$ along the [1 1 0] direction. The density functional calculations are well agreement with the experiment. As can be seen from Fig. 4(e) and (f), gKNB model can simultaneously provide the correct direction and the accurate magnitude of the polarization. Thus, the polarization induced by the triangular lattice spin order can be well explained by the general spin current term.

4.3. The spin order induced improper ferroelectric polarization in $BiFeO_3$

$BiFeO_3$ [56–58] is a well-known room-temperature multiferroic. Its ground state structure adopts a R3c space group with a large polarization ($\sim 100\ \mu C/cm^2$) [59] when the temperature is lower than the FE curie temperature T_C = 1000 K. Below the Neel temperature T_N = 650 K, a G-type AFM order with a long period incommensurate modulation takes place. Furthermore, some experiments reported the ME coupling in $BiFeO_3$. However, how magnetoelectric coupling actually occurs on a microscopic level in multiferroic $BiFeO_3$ is not clear. Then, we applied our unified model to investigate the origin of the ME coupling in $BiFeO_3$ [30]. We now turn to examine how the magnetoelastic coupling influences the electric polarization in $BiFeO_3$. By solving the formula in Part 3, we find that the strain is $\eta = (-8.26, -8.26, -35.58, 0, 0, 0)$ in the order of 10^{-4} as a result of the G-AFM ordering. Mediated by the coupling between the polarization and strain, the lattice change will induce a polarization. As can be seen in Table 1, our model predicts a lattice-deformation contribution to the polarization with a value of $P = 1.32\ \mu C/cm^2$, which is even larger than the sum of the pure electronic and ion displacement

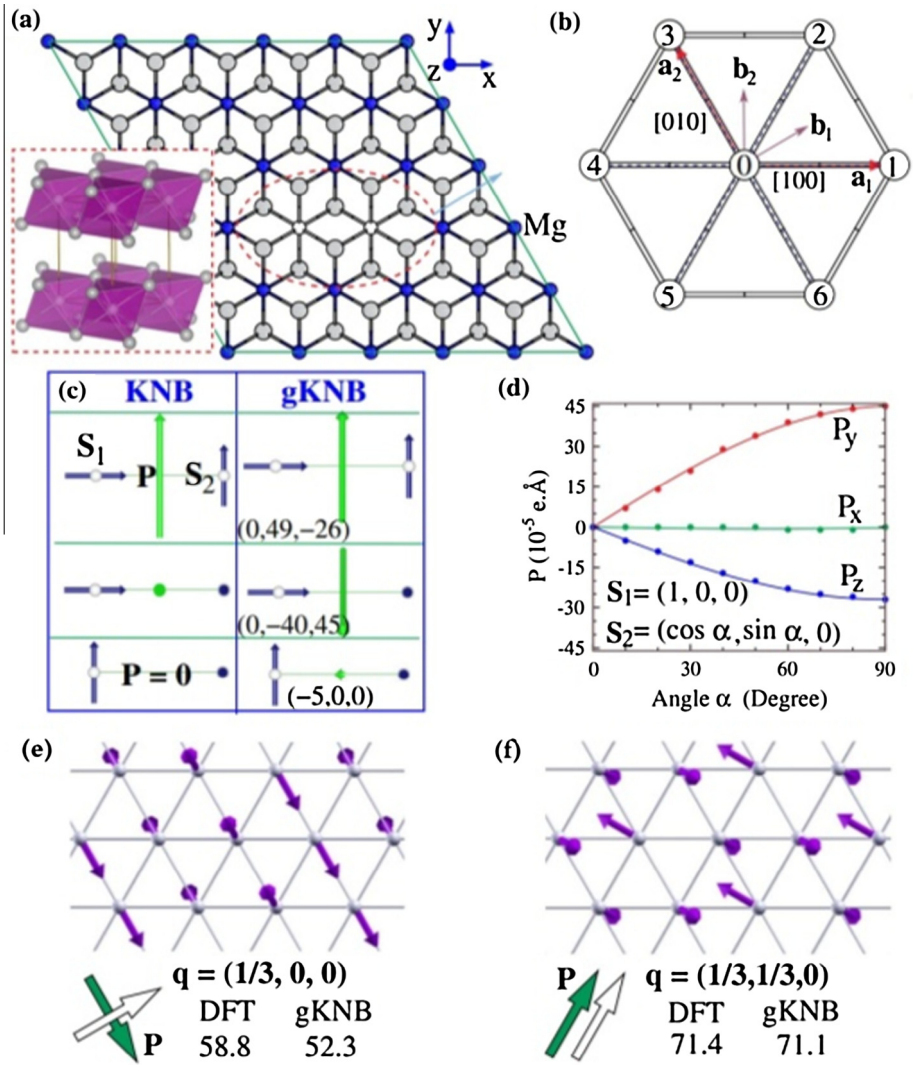

Fig. 4. (a) The $5 \times 5 \times 1$ supercell of MnI_2. The left inset illustrates the layered structure of MnI_2. (b) The triangular lattice of Mn^{2+} ions. (c) The electric polarizations predicted by the KNB and gKNB models for three different spin configurations of the Mn-Mn dimer. (d) The polarization of the Mn–Mn pairs extracted by the gKNB model (line) and direct density functional calculation (dot). (e and f). The spin orientations of two proper screw spirals with $\vec{q} = (\frac{1}{3}, 0, 0)$ and $\vec{q} = (\frac{1}{3}, \frac{1}{3}, 0)$ [33]. © 2011 American Physical Society.

contributions. This is an unprecedented result in which a previously unknown spin-order induced contribution to the electric polarization is found to be even larger than the widely known contributions. Table 1 also shows that the result obtained from our model is in agreement with the direct DFT calculations. Summing up all the three spin-order induced contributions shown in Table 1, the total polarization calculated for the G-type AFM order in BFO reaches $\sim 2\mu C/cm^2$. The spin-induced polarization in BFO is also comparable with that of $HoMnO_3$. Moreover, we find that the direction of the polarization caused by the spin order is opposite to the inherent electric polarization due to the R3c distortion. This is consistent with a recent experimental observation. In the experiment, the ion-displacement contribution deduced from the displacement of the Fe ions was determined to be $0.4\ \mu C/cm^2$ that is close to the value ($0.56\ \mu C/cm^2$) obtained from our model.

Table 1
The different contributions to the electric polarization (in units of $\mu C/cm^2$) induced by the G-AFM order in $BiFeO_3$ from the model and DFT calculations [30].

Polarization	$P_{lattice}$	P_e	P_{ion}
Model	1.32	0.53	0.56
DFT	1.22	0.40	0.54

5. Summary

In this article, we review the mechanisms of spin order induced improper ferroelectric polarization. We first outlined the previous polarization models (e.g., KNB model, inverse DM interaction model, exchange striction model, and bond polarization model) discussed in the literature. We then discuss our unified model in detail, which contains the pure electronic, ion displacement and the lattice deformation contributions in a unified framework. The previous models are the special cases of this unified model. This unified model is general and is able to explain the spin order induced ferroelectric polarization in almost all multiferroics. New multiferroics with strong magnetoelectric coupling and large polarization may be designed and/or predicted on the basis of this unified model.

Acknowledgements

Work at Fudan was supported by NSFC, FANEDD, NCET-10-0351, Research Program of Shanghai Municipality and MOE, the Special Funds for Major State Basic Research, Program for Professor of Special Appointment (Eastern Scholar), and Fok Ying Tung

Education Foundation. H.X. thanks Prof. M.-H. Whangbo, Prof. S.-H. Wei, Prof. S. Dong, Prof. E.J. Kan for the collaborations.

Appendix A. Four-states mapping method for computing coefficients of pure electronic part of the unified model

The electronic contribution of polarization for a spin dimer is: $\vec{P} = \vec{P}_1(\vec{S}_1) + \vec{P}_2(\vec{S}_2) + \vec{P}_{12}(\vec{S}_1, \vec{S}_2)$, where $\vec{P}_i(\vec{S}_i) = \vec{P}_i^{xx}S_{ix}^2 + \vec{P}_i^{yy}S_{iy}^2 + \vec{P}_i^{zz}S_{iz}^2 + 2\vec{P}_i^{xy}S_{ix}S_{iy} + 2\vec{P}_i^{xz}S_{ix}S_{iz} + 2\vec{P}_i^{yz}S_{iy}S_{iz}$. Considering that $\vec{P}_{12}(\vec{S}_1, \vec{S}_2) = -\vec{P}_{12}(-\vec{S}_1, \vec{S}_2)$, we extract the polarization coefficients as follows:

A.1. single site term

(1) For $\vec{P}_i^{xy}$, we can use the following spin arrangements:

$$\text{I}: \ \vec{S}_i = \left(\frac{\sqrt{2}}{2}, \frac{\sqrt{2}}{2}, 0\right)$$
$$\text{II}: \ \vec{S}_i = \left(\frac{\sqrt{2}}{2}, -\frac{\sqrt{2}}{2}, 0\right)$$
$$\text{III}: \ \vec{S}_i = \left(-\frac{\sqrt{2}}{2}, \frac{\sqrt{2}}{2}, 0\right)$$
$$\text{IV}: \ \vec{S}_i = \left(-\frac{\sqrt{2}}{2}, -\frac{\sqrt{2}}{2}, 0\right)$$

The magnetic order of other magnetic ions is set according to the experimental states and remains unchanged during the four calculations. And one can easily obtain that $\vec{P}_i^{xy} = \frac{\vec{P}_{\text{I}} + \vec{P}_{\text{IV}} - \vec{P}_{\text{II}} - \vec{P}_{\text{III}}}{4}$.

(2) For $\vec{P}_i^{xz}$, we can use the following spin arrangements:

$$\text{I}: \ \vec{S}_i = \left(\frac{\sqrt{2}}{2}, 0, \frac{\sqrt{2}}{2}\right)$$
$$\text{II}: \ \vec{S}_i = \left(\frac{\sqrt{2}}{2}, 0, -\frac{\sqrt{2}}{2}\right)$$
$$\text{III}: \ \vec{S}_i = \left(-\frac{\sqrt{2}}{2}, 0, \frac{\sqrt{2}}{2}\right)$$
$$\text{IV}: \ \vec{S}_i = \left(-\frac{\sqrt{2}}{2}, 0, -\frac{\sqrt{2}}{2}\right)$$

As in case (1), one can easily obtain that $\vec{P}_i^{xz} = \frac{\vec{P}_{\text{I}} + \vec{P}_{\text{IV}} - \vec{P}_{\text{II}} - \vec{P}_{\text{III}}}{4}$.

(3) For $\vec{P}_i^{yz}$, we can use the following spin arrangements:

$$\text{I}: \ \vec{S}_i = \left(0, \frac{\sqrt{2}}{2}, \frac{\sqrt{2}}{2}\right)$$
$$\text{II}: \ \vec{S}_i = \left(0, \frac{\sqrt{2}}{2}, -\frac{\sqrt{2}}{2}\right)$$
$$\text{III}: \ \vec{S}_i = \left(0, -\frac{\sqrt{2}}{2}, \frac{\sqrt{2}}{2}\right)$$
$$\text{IV}: \ \vec{S}_i = \left(0, -\frac{\sqrt{2}}{2}, -\frac{\sqrt{2}}{2}\right)$$

As in case (1), one can easily obtain that $\vec{P}_i^{yz} = \frac{\vec{P}_{\text{I}} + \vec{P}_{\text{IV}} - \vec{P}_{\text{II}} - \vec{P}_{\text{III}}}{4}$.

(4) For the diagonal terms, we note that

$$\begin{aligned}\vec{P}_i^{xx}S_{ix}^2 + \vec{P}_i^{yy}S_{iy}^2 + \vec{P}_i^{zz}S_{iz}^2 &= \vec{P}_i^{xx}(1 - S_{iy}^2 - S_{iz}^2) + \vec{P}_i^{yy}S_{iy}^2 + \vec{P}_i^{zz}S_{iz}^2 \\ &= \vec{P}_i^{xx} + (\vec{P}_i^{yy} - \vec{P}_i^{xx})S_{iy}^2 + (\vec{P}_i^{zz} - \vec{P}_i^{xx})S_{iz}^2.\end{aligned}$$

For $\vec{P}_i^{yy} - \vec{P}_i^{xx}$, we can use the following four spin arrangements:

$$\text{I}: \ \vec{S}_i = (0, 1, 0)$$
$$\text{II}: \ \vec{S}_i = (0, -1, 0)$$
$$\text{III}: \ \vec{S}_i = (1, 0, 0)$$
$$\text{IV}: \ \vec{S}_i = (-1, 0, 0)$$

As in case (1), we can get $\vec{P}_i^{yy} - \vec{P}_i^{xx} = \frac{\vec{P}_{\text{I}} + \vec{P}_{\text{II}} - \vec{P}_{\text{III}} - \vec{P}_{\text{IV}}}{2}$.

For $\vec{P}_i^{zz} - \vec{P}_i^{xx}$, we can use the following four spin arrangements:

$$\text{I}: \ \vec{S}_i = (0, 0, 1)$$
$$\text{II}: \ \vec{S}_i = (0, 0, -1)$$
$$\text{III}: \ \vec{S}_i = (1, 0, 0)$$
$$\text{IV}: \ \vec{S}_i = (-1, 0, 0)$$

As in case (1), we can get $\vec{P}_i^{zz} - \vec{P}_i^{xx} = \frac{\vec{P}_{\text{I}} + \vec{P}_{\text{II}} - \vec{P}_{\text{III}} - \vec{P}_{\text{IV}}}{2}$.

To get the individual coefficients of the diagonal terms, we can enforce the condition $\vec{P}_i^{xx} + \vec{P}_i^{yy} + \vec{P}_i^{zz} = 0$, which removes the spin independent contribution. Note that the single site term is SOC related, so SOC is necessary in the calculations.

A.2. Exchange striction term

(5) The exchange striction interaction is independent on SOC effect, so to extract the coefficients $\vec{P}_{es}^{ij}$ one should exclude the SOC effect. One can use the following four spin arrangements:

I. up-spins for $\vec{S}_i$ and $\vec{S}_j$: $(\uparrow, \uparrow)$
II. up-spin for $\vec{S}_i$ and down-spin for $\vec{S}_j$: $(\uparrow, \downarrow)$
III. down-spin for $\vec{S}_i$ and up-spin for $\vec{S}_j$: $(\downarrow, \uparrow)$
IV. down-spins for $\vec{S}_i$ and $\vec{S}_j$: $(\downarrow, \downarrow)$

In these four spin arrangements, the spin orientations for the spin sites other than $\vec{S}_i$ and $\vec{S}_j$ are the same but can be arbitrary. We can get $\vec{P}_{es}^{ij} = \frac{\vec{P}_{\text{I}} + \vec{P}_{\text{IV}} - \vec{P}_{\text{II}} - \vec{P}_{\text{III}}}{4}$.

A.3. General spin current term

(6) Now we extract the coefficients of general spin current term $\vec{M}$.

To obtain the intersite polarization coefficient $\vec{P}_{ij}^{yz}$, we can calculate the electric polarizations of the following four spin arrangements:

$$\text{I}: \ \vec{S}_i = (0, 1, 0); \ \vec{S}_j = (0, 0, 1)$$
$$\text{II}: \ \vec{S}_i = (0, 1, 0); \ \vec{S}_j = (0, 0, -1)$$
$$\text{III}: \ \vec{S}_i = (0, -1, 0); \ \vec{S}_j = (0, 0, 1)$$
$$\text{IV}: \ \vec{S}_i = (0, -1, 0); \ \vec{S}_j = (0, 0, -1)$$

The others are set according to the experimental spin states and remain unchanged during the four calculations. We can get $\vec{P}_{ij}^{yz} = \frac{\vec{P}_{\text{I}} + \vec{P}_{\text{IV}} - \vec{P}_{\text{II}} - \vec{P}_{\text{III}}}{4}$.

To obtain the intersite polarization coefficient $\vec{P}_{ij}^{zx}$, we can calculate the electric polarizations of the following four spin arrangements:

$$\text{I}: \ \vec{S}_i = (0,0,1);\ \vec{S}_j = (1,0,0)$$
$$\text{II}: \ \vec{S}_i = (0,0,1);\ \vec{S}_j = (-1,0,0)$$
$$\text{III}: \ \vec{S}_i = (0,0,-1);\ \vec{S}_j = (1,0,0)$$
$$\text{IV}: \ \vec{S}_i = (0,0,-1);\ \vec{S}_j = (-1,0,0)$$

The others are set according to the experimental spin states and remain unchanged during the four calculations. We can get $\vec{P}_{ij}^{zx} = \frac{\vec{P}^{I} + \vec{P}^{IV} - \vec{P}^{II} - \vec{P}^{III}}{4}$.

To obtain the intersite polarization coefficient $\vec{P}_{ij}^{xy}$, we can calculate the electric polarizations of the following four spin arrangements:

$$\text{I}: \ \vec{S}_i = (1,0,0);\ \vec{S}_j = (0,1,0)$$
$$\text{II}: \ \vec{S}_i = (1,0,0);\ \vec{S}_j = (0,-1,0)$$
$$\text{III}: \ \vec{S}_i = (-1,0,0);\ \vec{S}_j = (0,1,0)$$
$$\text{IV}: \ \vec{S}_i = (-1,0,0);\ \vec{S}_j = (0,-1,0)$$

The others are set according to the experimental spin states and remain unchanged during the four calculations. We can get $\vec{P}_{ij}^{xy} = \frac{\vec{P}^{I} + \vec{P}^{IV} - \vec{P}^{II} - \vec{P}^{III}}{4}$.

The general spin current term originates from SOC effect. It is necessary to include the SOC effect during the calculation. Note that in the general cases (no inversion symmetry in the spin dimer) all the coefficients of the intersite polarization should be fitted. In most cases, the anisotropic term is small thus can be neglected.

References

[1] S.-W. Cheong, M. Mostovoy, Nature Mater. 6 (2007) 13.
[2] R. Ramesh, N. Spaldin, Nature Mater. 6 (2007) 21.
[3] S. Picozzi, C. Ederer, J. Phys.: Condens. Matter 21 (2009) 303201.
[4] K.F. Wang, J.-M. Liu, Z. Ren, Adv. Phys. 58 (2009) 321.
[5] J. van den Brink, D. Khomskii, J. Phys.: Conders. Matter 20 (2008) 434217.
[6] Y. Tokura, S. Seki, Adv. Mater. 22 (2010) 1554.
[7] J. Ma, J.M. Hu, Z. Li, C.W. Nan, Adv. Mater. 23 (2011) 1062.
[8] C.W. Nan, M.I. Bichurin, S. Dong, D. Viehland, G. Srinivasan, J. Appl. Phys. 103 (2008) 031101.
[9] S. Zhang, Y.G. Zhao, P.S. Li, J.J. Yang, S. Rizwan, J.X. Zhang, J. Seidel, T.L. Qu, Y.J. Yang, Z.L. Luo, Q. He, T. Zou, Q.P. Chen, J.W. Wang, L.F. Yang, Y. Sun, Y.Z. Wu, X. Xiao, X.F. Jin, J. Huang, C. Gao, X.F. Han, R. Ramesh, Phys. Rev. Lett. 108 (2012) 137203.
[10] C.-G. Duan, S.S. Jaswal, E.Y. Tsymbal, Phys. Rev. Lett. 97 (2006) 047201.
[11] J.T. Heron, M. Trassin, K. Ashraf, M. Gajek, Q. He, S.Y. Yang, D.E. Nikonov, Y.-H. Chu, S. Salahuddin, R. Ramesh, Phys. Rev. Lett. 107 (2011) 217202.
[12] V. Garcia, M. Bibes, L. Bocher, S. Valencia, F. Kronast, A. Crassous, X. Moya, S. Enouz-Vedrenne, A. Gloter, D. Imhoff, C. Deranlot, N.D. Mathur, S. Fusil, K. Bouzehouane, A. Barthelemy, Science 327 (2010) 1106–1110.
[13] D. Khomskii, Physics 2 (2009) 20.
[14] M.-R. Li, P.W. Stephens, M. Retuerto, T. Sarkar, C.P. Grams, J. Hemberger, M.C. Croft, D. Walker, M. Greenblatt, J. Am. Chem. Soc. 136 (2014) 8508–8511;
P.S. Wang, W. Ren, L. Bellaiche, H.J. Xiang, Phys. Rev. Lett. 114 (2015) 147204.
[15] R.V. Shpanchenko, V.V. Chernaya, A.A. Tsirlin, P.S. Chizhov, D.E. Sklovsky, E.V. Antipov, E.P. Khlybov, V. Pomjakushin, A.M. Balagurov, J.E. Medvedeva, E.E. Kaul, C. Geibel, Chem. Mater. 16 (2004) 3267–3273.
[16] S.V. Kiselev, R.P. Ozerov, G.S. Zhdanov, Sov. Phys. Dokl. 7 (1963) 742.
[17] R. Seshadri, N.A. Hill, Chem. Mater. 13 (9) (2001) 2892.
[18] B.B. Van Aken, T.T.M. Palstra, A. Filippetti, N.A. Spaldin, Nat. Mater. 3 (2004) 164.
[19] T. Kimura, T. Goto, H. Shintani, K. Ishizaka, T. Arima, Y. Tokura, Nature 6 (2003) 426;
H.J. Xiang, Su-Huai Wei, M.-H. Whangbo, Juarez L.F. Da Silva, Phys. Rev. Lett. 101 (2008) 037209.
[20] O. Prokhnenko, R. Feyerherm, E. Dudzik, S. Landsgesell, N. Aliouane, L.C. Chapon, D.N. Argyriou, Phys. Rev. Lett. 98 (2007) 057206.
[21] N. Hur, S. Park, P.A. Sharma, J.S. Ahn, S. Guha, S.-W. Cheong, Nature (London) 429 (2004) 392.
[22] G. Zhang, S. Dong, Z. Yan, Y. Guo, Q. Zhang, S. Yunoki, E. Dagotto, J.-M. Liu, Phys. Rev. B 84 (2011) 174413.
[23] R.D. Johnson, L.C. Chapon, D.D. Khalyavin, P. Manuel, P.G. Radaelli, C. Martin, Phys. Rev. Lett. 108 (2012) 067201.
[24] H. Katsura, N. Nagaosa, A. Balatsky, Phys. Rev. Lett. 95 (2005) 057205.
[25] I.A. Sergienko, E. Dagotto, Phys. Rev. B 73 (2006) 094434.
[26] I.A. Sergienko, C. Sen, E. Dagotto, Phys. Rev. Lett. 97 (2006) 227204.
[27] C. Jia, S. Onoda, N. Nagaosa, J.H. Han, Phys. Rev. B 74 (2006) 224444.
[28] M. Mostovoy, Phys. Rev. Lett. 96 (2006) 067601.
[29] H.J. Xiang, P.S. Wang, M.-H. Whangbo, X.G. Gong, Phys. Rev. B 88 (2013) 054404.
[30] X.Z. Lu, Xifan Wu, H.J. Xiang, Phys. Rev. B 91 (2015) 100405(R).
[31] H.J. Xiang, E.J. Kan, Su-Huai Wei, M.-H. Whangbo, X.G. Gong, Phys. Rev. B 84 (2011) 224429.
[32] J.H. Yang, Z.L. Li, X.Z. Lu, M.-H. Whangbo, Su-Huai Wei, X.G. Gong, H.J. Xiang, Phys. Rev. Lett. 109 (2013) 107203.
[33] H.J. Xiang, E.J. Kan, Y. Zhang, M.-H. Whangbo, X.G. Gong, Phys. Rev. Lett. 107 (2011) 157202.
[34] X.Z. Lu, M.-H. Whangbo, Shuai Dong, X.G. Gong, H.J. Xiang, Phys. Rev. Lett. 108 (2012) 187204.
[35] M. Kenzelmann, A.B. Harris, S. Jonas, C. Broholm, J. Schefer, S.B. Kim, C.L. Zhang, S.-W. Cheong, O.P. Vajk, J.W. Lynn, Phys. Rev. Lett. 95 (2005) 087206.
[36] T. Kurumaji, S. Seki, S. Ishiwata, H. Murakawa, Y. Tokunaga, Y. Kaneko, Y. Tokura, Phys. Rev. Lett. 106 (2011) 167206.
[37] T. Kimura, J.C. Lashley, A.P. Ramirez, Phys. Rev. B 73 (2006) 220401(R).
[38] S. Seki, Y. Yamasaki, Y. Shiomi, S. Iguchi, Y. Onose, Y. Tokura, Phys. Rev. B 75 (2007) 100403(R).
[39] S. Seki, Y. Onose, Y. Tokura, Phys. Rev. Lett. 101 (2008) 067204.
[40] I. Dzialoshinski, J. Phys. Chem. Solids 4 (1958) 241.
[41] T. Moriya, Phys. Rev. 120 (1960) 91.
[42] T. Arima, T. Goto, Y. Yamasaki, S. Miyasaka, K. Ishii, M. Tsubota, T. Inami, Y. Murakami, Y. Tokura, Phys. Rev. B 72 (2005) 100102(R).
[43] T. Arima, J. Phys. Soc. Jpn. 76 (2007) 073702.
[44] H. Murakawa, Y. Onose, S. Miyahara, N. Furukawa, Y. Tokura, Phys. Rev. Lett. 105 (2010) 137202.
[45] K. Yamauchi, P. Barone, S. Picozzi, Phys. Rev. B 84 (2011) 165137.
[46] S. Picozzi, K. Yamauchi, B. Sanyal, I.A. Sergienko, E. Dagotto, Phys. Rev. Lett. 99 (2007) 227201.
[47] B. Lorenz, Y.-Q. Wang, C.-W. Chu, Phys. Rev. B. 76 (2007) 104405.
[48] Y.J. Choi, H.T. Yi, S. Lee, Q. Huang, V. Kiryukhin, S.-W. Cheong, Phys. Rev. Lett. 100 (2008) 047601.
[49] Y. Zhang, H.J. Xiang, M.-H. Whangbo, Phys. Rev. B 79 (2009) 054432.
[50] C. Wang, G.-C. Guo, L. He, Phys. Rev. Lett. 99 (2007) 177202.
[51] D. Dai, H.J. Xiang, M.-H. Whangbo, J. Comput. Chem. 29 (2008) 2187.
[52] H.J. Xiang, C. Lee, H.-J. Koo, X.G. Gong, M.-H. Whangbo, Dalton Trans. 42 (2013) 823.
[53] X. Wu, D. Vanderbilt, D.R. Hamann, Phys. Rev. B 72 (2005) 035105.
[54] C.W. Swartz, X. Wu, Phys. Rev. B 85 (2012) 054102.
[55] J.C. Wojdel, J. Iniguez, Phys. Rev. Lett. 103 (2009) 267205.
[56] J.R. Teague, R. Gerson, W. James, Solid State Commun. 8 (1970) 1073.
[57] I. Sosnowska, T.P. Neumaier, E. Steichele, J. Phys. C 15 (1982) 4835.
[58] R.D. Johnson, P. Barone, A. Bombardi, R.J. Bean, S. Picozzi, P.G. Radaelli, Y.S. Oh, S.-W. Cheong, L.C. Chapon, Phys. Rev. Lett. 110 (2013) 217206.
[59] J. Wang, J.B. Neaton, H. Zheng, V. Nagarajan, S.B. Ogale, B. Liu, D. Viehland, V. Vaithyanathan, D.G. Schlom, U.V. Waghmare, N.A. Spaldin, K.M. Rabe, M. Wuttig, R. Ramesh, Science 299 (2003) 1719–1722.